Available online at www.sciencedirect.com

ScienceDirect

Procedia Manufacturing 47 (2020) 202–208

Procedia MANUFACTURING

www.elsevier.com/locate/procedia

23rd International Conference on Material Forming (ESAFORM 2020)

FEM Validation of Front End and Back End Defects Evolution in AA6063 and AA6082 Aluminum Alloys Profiles

Marco Negozio[a,]*, Riccardo Pelaccia[b], Lorenzo Donati[a], Barbara Reggiani[b], Luca Tomesani[a], Tommaso Pinter[c]

[a]*DIN- Department of Industrial Engineering, University of Bologna, Viale Risorgimento 2, 40133, Bologna, Italy*
[b]*DISMI- Department of Sciences of Methods for Engineering, University of Modena and Reggio Emilia, Viale Amendola 2, 42124, Reggio Emilia, Italy*
[c]*Almax Mori, Via Matteotti 13, 38065, Mori, Italy*

* Corresponding author. Tel.: +390512090496; *E-mail address:* marco.negozio2@unibo.it

Abstract

The reduction of scraps related to back end defects (i.e. billet skin contamination) and front end defects (i.e. charge welds) is gaining nowadays an increasing industrial interest in order to obtain greater process efficiency. Today, extrusion industrial practice faces the issue by means of technician's experience, empirical rules or, in most critical profiles, through time consuming and expensive experimental analyses. On the other side, FEM simulation of extrusion dies is becoming a common support tool for the design of new critical dies. Stating this scenario, the possibility to include the prediction of front end and back end defects evolution as simulation output can then be easily obtained at almost comparable computational costs. In this paper the FEM code Altair HyperXtrude® is used for the simulation of 2 industrial cases made by AA6063 and AA6082 alloys following the transient moving boundaries approach. Experimentally, the profiles were extruded, sectioned, polished and etched with caustic soda in order to reveal and measure front and back end development in front of and behind the profile stop mark. The data obtained from experimental analyses are initially discussed referring to billet skin contamination and charge weld evolution, then compared to industrial experience, to theoretical and empirical methods available in literature and to FEM results in order to evaluate pros and cons of each evaluation method.

Keywords: Extrusion; Aluminum Alloys; FEM simulation; Charge Welds; Skin

1. Introduction

Extrusion of aluminum alloys represents an economic manufacturing process that allows the production of complex profiles maintaining a high level of quality in terms of mechanical properties. In the profile, at the beginning and end of each extruded billet, these properties are influenced by the presence of defects caused by the nature of the process or by the die design and the process parameters. Such defects, known as front end and back end defects, require scrapping of the extruded profile in which they are present. The first one, also known as "Charge Welds", occurs at the start of each press cycle as consequence of the presence of oxides or impurities (dust, lubricant, etc.) in the welding area between two consecutive billets. In Fig.1, an example of charge weld evolution is schematized: the darker area refers to the new billet, the bright one to the old billet. Whenever there is presence of both new and old billet material in the same section of the profile (Fig. 1 b and c in section A-A) a loss of mechanical properties occurs [1]. It is not possible to avoid charge welds in the profile because they are caused by the nature of the direct extrusion process. The second type of defect, also known as "Billet Skin Contamination", is related to the outer layer of the billets. The outer layer has a different chemical composition and microstructure with respect to the base billet material [2] as consequence of the DC-casting

10.1016/j.promfg.2020.04.178

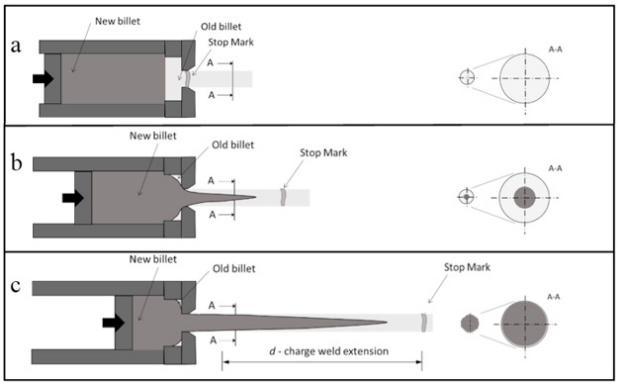

Fig. 1. Schematic view of the charge weld evolution for a round solid bar: (a) beginning of the process stroke, (b) charge weld formation, (c) charge weld extension.

process and it also usually contains several contaminations as oxides, dust or impurities, collected during the billet handling and pre-heating. During deformation, the billet skin can flow inside the die until it reaches the extruded profile, thus generating a drastic decrease of the mechanical proprieties.
The skin contamination can be controlled through the length of the billet rest: if the billet rest is too short, skin flows inside the profile even before the stop mark (Fig. 2a) thus generating the discard of some meters of profile extruded on the right hand side of the stop mark. If it is too long, there is no contamination on the profile but too much billet material is discarded in the billet rest (Fig.2b). Fig. 2c represents the optimal condition where there is no billet skin contamination in the profile and a minimal thickness of the billet rest.

The experimental determination of charge welds and skin contamination along the extruded profile is a time consuming analysis, requiring several phases such as cutting, marking, grinding, polishing and etching for, usually, a big number of samples, and where the results can be referred only to that particular geometry. Such analysis is conducted only when mandatory required by the customer whilst, for standard profile, internal empirical rules are usually adopted.

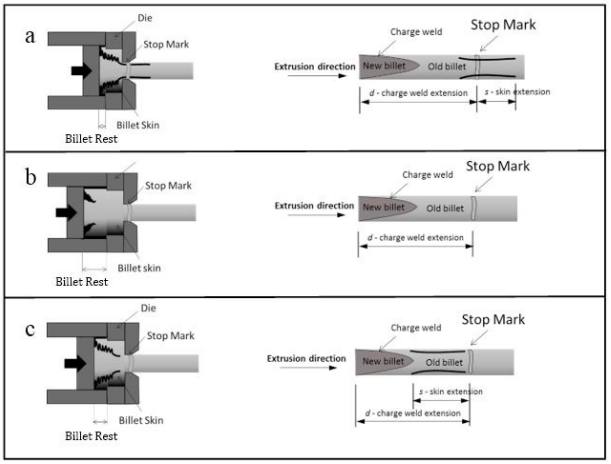

Fig. 2. Schematic view of the skin contamination evolution for a solid bar: (a) too short rest, (b) too long rest, (c) optimal billet rest.

Indeed, in industrial practice, it is frequent to discard 1000 mm before the stop mark for skin contamination and, for the charge weld, 1000 to 3000 mm after the stop mark in relation to the profile extrusion ratio R: for R<30 1000 mm, for 30<R<40 2000 mm, for R>40 3000 mm [3].

Concerning the theory of charge welds extent estimation, some studies are available in literature for the prediction of this defect but, to the best author's knowledge, only two theoretical formulae (1) (2) have been proposed [4, 11]:

$$d = \frac{(V1 + V2)}{Ae \times n} \tag{1}$$

where the charge weld extent (d) has been related to the volume of material present in the die ports ($V1$), to the volume of material present in the welding chambers ($V2$), to the exit profile section area (Ae) and to the number of the profile openings in the die (n);

$$d = 1.5 \times \frac{(V1 + V2)}{Ae \times n} \tag{2}$$

in (2), a corrective factor 1.5 has been introduced to better match experimental trials, as reported in [11], as result of two consideration: on one hand, the metal leaving the die at the start of the next billet extrusion is not the entire port volume (it can vary from the 60% to the 90% of it, and this is mainly due to the presence of dead metal zones). On the other hand, the flow of the material is faster in the center of the ports, with a gradual clearing towards the outside. These formulae are often used for a fast computation of the defect development, but their accuracy has not been extensively evaluated yet. Recently, FE codes have been implemented for the prediction of the charge welds evolution, providing a good correlation between experimental and numerical simulation [5-8].

Concerning skin contamination, the defect evolution has been investigated mainly by experiments [9-11], or by 2D simulations [12, 13]. One study was performed in order to investigate experimentally the influence of process parameters on skin evolution [14], while only one paper tried to compare the outputs of numerical simulations with experimental data on an extruded profile with a complex geometry [15], but the comparison was made on the billet discard and not on the evolution in the profile.

To the best author's knowledge, only one empirical formula (3) has been reported in literature by Jowett et al. [11] for skin contamination length prediction:

$$s = \frac{(14\% \times Vb - 75\% \times (V1 + V2) - Vrest)}{Ae \times n} \tag{3}$$

where Vb and $Vrest$ are the billet and the billet rest volume respectively, and the other terms follow the definitions used in equations (1) and (2).

Numerical simulation is today a mandatory tool for leader manufacturers of extrusion dies due to the possibility to optimize them directly at the design stage in terms of conflicting requirements (material flow balancing, seam weld quality, die life, etc), reducing, consequently, the die trials and global manufacturing lead times. The opportunity to include also the prediction of the front-end and back-end defects in the die design optimization stage is, consequently, of high

relevance to companies, in particular if such analysis can be performed in conjunction with conventional analyses, without the need of running multiple simulations.

Aim of this study is to experimentally investigate the evolution of charge welds and skin contamination in two industrial cases, extruding alloys AA6063 and AA6082 and to evaluate the accuracy of the FEM prediction by means of Altair HyperXtrude numerical simulations in relation also to the theoretical and empirical formulae available in literature.

2. Experimental investigation

The geometries of the profiles under investigation are reported in Fig.3. Both profiles are solid (absence of seam welds): profile 1, made by AA6082 alloy, is produced by a flat die with a single die opening whilst profile 2, made by AA6063 alloy, is produced by means a flat two-hole die.

The two profiles are produced by Indinvest LT plant of Latina (Italy): each production batch involves the processing of around 50 consecutive billets. The analyzed samples come from the transition from the sixth to the seventh billets of each relative cycle in order to have steady-state conditions in the tool-die set.

The two extruded profiles were initially cut into 100 mm length samples adjacent to the stop mark. Every selected sample was analyzed in order to obtain experimental data of charge welds and skin contamination evolution. Every sample was grinded with P220 and P500 abrasive papers. Then a caustic soda etching (30% NaOH for 1 liter of H_2O heated to 60 °C, etching time from 45 to 90 seconds) was made in order to reveal skin contamination and charge welds (Fig. 4). Finally, images of profile's section were scanned and data related to defects development were collected.

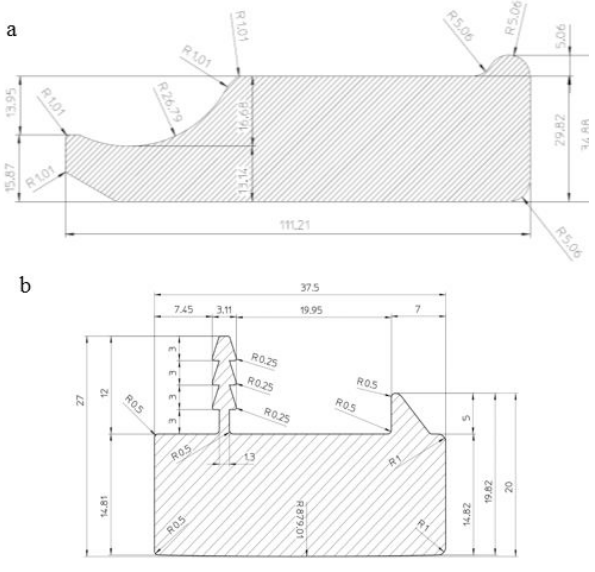

Fig. 3. Geometries under investigation: (a) profile 1, (b) profile 2.

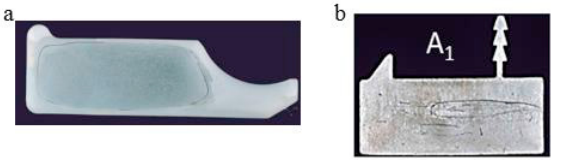

Fig. 4. Geometries investigated after etching: (a) profile 1, (b) profile 2.

2.1. Process parameters and experimental results

In Tab.1 process parameters used in the extrusion of the analyzed industrial cases are reported.

To evaluate the thickness of the billet skin, a slice of one billet (one for each analyzed profile) was taken from the same experimental batch, then grinded and etched (Fig. 5): a value of 250 microns was found for both alloys.

Table 1. Process parameters and geometry tolerances.

Process Parameters and geometry tolerances	Profile 1	Profile 2
Aluminum alloy	AA6082	AA6063
Ram speed [mm/s]	7.64	6.44
Container temperature [°C]	440	430
Billet temperature [°C]	530	530
Die temperature [°C]	450	450
Ram acceleration time [s]	5	5
Extrusion ratio	20	44
Billet length [mm]	990	670
Billet diameter [mm]	254	260
Container diameter [mm]	266	264
Billet Rest length [mm]	15	15
Skin thickness [µm]	250	250

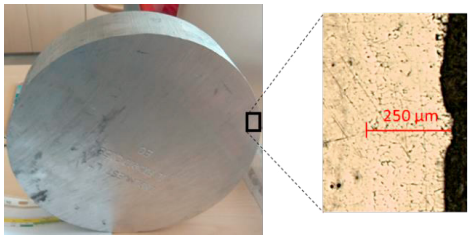

Fig. 5. Billet skin layer.

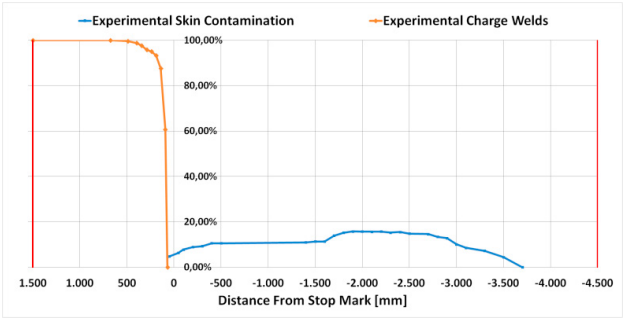

Fig. 6. Profile 1: charge welds (orange) and skin contamination (blue) evolutions. Vertical red lines represent the scrap realized by the company based on internal experience.

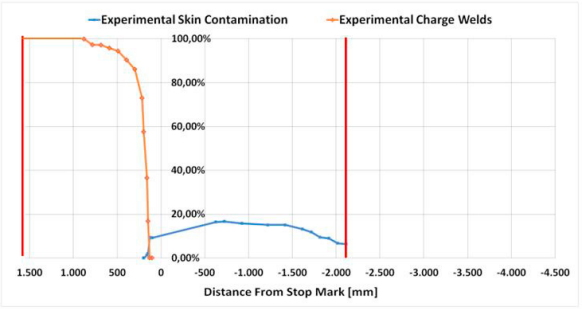

Fig. 7. Profile 2: charge welds (orange) and skin contamination (blue) evolutions. Vertical red lines represent the scrap realized by the company based on internal experience.

The images acquired after etching were elaborated in order to reconstruct the evolution of billet skin and charge welds along the extruded profile length using the stop mark as reference point. Fig. 6 and Fig. 7 report the development of skin contamination and charge welds within the profile section at different distances from stop mark: negative values on x-axis represent samples extracted from the end of the billet 6 (back-end defect) whilst positive ones represent samples extracted from the transition from billet 6th to 7th (front-end defect).

Vertical lines, in red in the figures, represent the extremes of the scrap made by the company (the discarded part is between the two lines), based on the technician's experience.

As depicted by the figures an un-optimized amount of extruded profile length is discarded: sometimes the scrap is longer than the defects extension (Fig 6: both front and rear; Fig. 7: front), sometimes the scrap is not enough (Fig. 7: rear).

Concerning the charge welds, both profiles show a similar evolution of the defect contamination (Figures 8 and 10): in profile 1 it appears after 70 mm from the stop mark, reaching the 95 % of contamination after 250 mm and the 99,5% after 500 mm. In profile 2, charge welds appears after 130 mm, reaching the 95% after 580 mm and the 99,5% after 900 mm. In both cases the contamination grows fast just after the start of the defect, and then progressively slows down approaching the 99,5% material replacement. Almost in both profiles, in the first 50% of the defect extent, the contamination increases from 0% to 95% while, in the other 50%, it grows from 95% to 99,5%.

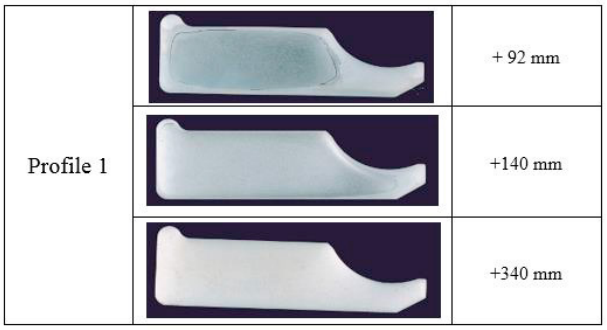

Fig. 8. Charge welds evolution on profile 1 at different distances from the stop mark.

Concerning the billet skin contamination, it does not evolve up to 100% on the profile section (as clearly evidenced in Figures 6, 7, 9 and 11) but rather the contaminated section remains roughly constant during ram stroke. The contamination appears almost at the end of the ram stroke (i.e. distance from the stop mark, -3700 mm in profile 1), it enlarges up to a certain value (i.e. 15-20% at -900 mm in Fig. 9) and remains nearly constant for the remaining stroke (i.e. -200 mm in Fig. 9). At this point, the contamination is slightly reduced (below 10 % at +50 mm distance from stop mark) and, approaching the charge welds, it flattens and evolves with them up to the 100% material replacement.

In order to better understand the evolution between billet skin contamination and charge weld, the profile 1 was also sectioned in the middle of the profile in the longitudinal direction (Fig. 12). The skin contamination is stable for a certain length in the middle of the profile, then it is thinned and shifted towards one side by the approaching of the charge welds interface. Billet skin contamination ends directly over the charge welds line, then evolves with them to a full section replacement.

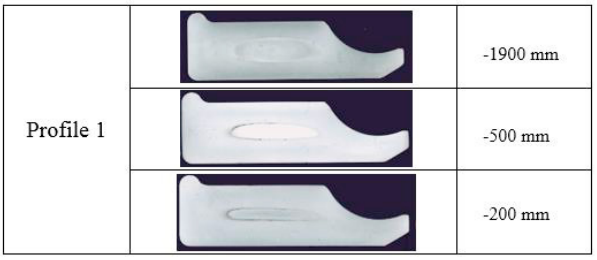

Fig. 9. Skin contamination evolution on profile 1 at different distances from the stop mark.

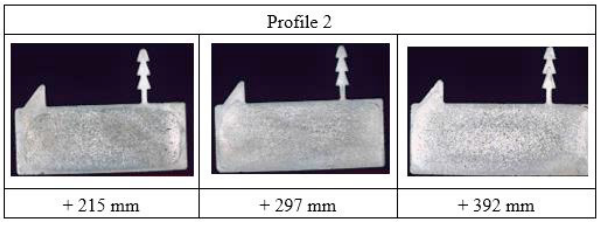

Fig. 10. Charge welds evolution on profile 2 at different distances from the stop mark.

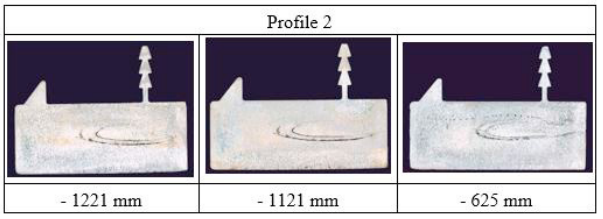

Fig. 11. Skin contamination evolution on profile 2 at different distances from the stop mark.

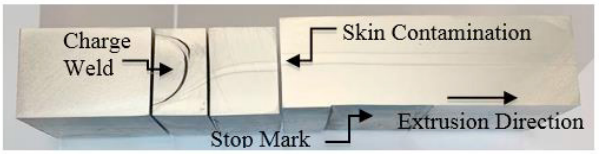

Fig. 12. Skin behavior at the point in which charge welds appears.

3. Numerical and analytical investigation

3.1. Numerical setup

Numerical simulations of the two industrial cases were made by means of FE code HyperXtrude® by Altair Engineering (Fig. 13). Starting from the 3D CAD models, through Boolean subtraction, material flow geometries were obtained in order to perform Arbitrarian Lagrangian Eulerian transient simulations.

The following simulation parameters were used:

- billet, feeder, porthole and pockets components meshed with 3D tetrahedral 4-noded elements;
- bearing and profile regions meshed with 3D prismatic 6-nodes elements;
- viscoplastic friction model with a coefficient value of 0,3;
- convective coefficient of 3000 W/(m^2*°C) for the workpiece / tool interfaces;
- zero normal stress boundary condition at the exit of the die;
- Hensel-Spittel plastic flow constitutive model [16] was used (4), where $\bar{\sigma}$ is the flow stress, $\bar{\varepsilon}$ the strain, $\dot{\bar{\varepsilon}}$ the strain rate, T the temperature (°K). Tab. 3 reports the Hensel-Spittel coefficients used in the simulations, as determined for the two alloys in previous works [17-18];
- HyperXtrude® code allows the simulation of the skin contamination evolution, by defining the initial value of the skin thickness in the billet; therefore, as reported in Tab. 1, this value was set on 250 µm for the two billets.

$$\bar{\sigma} = A \cdot e^{m_1 T} \cdot \bar{\varepsilon}^{-m_2} \cdot \dot{\bar{\varepsilon}}^{-m_3} \cdot e^{\frac{m_4}{\bar{\varepsilon}}} \cdot (1+\bar{\varepsilon})^{m_5 T} \cdot e^{m_7 \bar{\varepsilon}} \cdot \dot{\bar{\varepsilon}}^{m_8 T} \cdot T^{m_9} \quad (4)$$

Table 3. Hensel-Spittel parameters.

Hensel-Spiettel Parameters	Profile 1	Profile 2
A [MPa]	568000	1135.82
m1 [K^{-1}]	-0.002117	-0.004784
m2	0.1059	0.077934
m3	0.08299	-0.225984
m4	0.0009266	0.00197
m5 [K^{-1}]	-0.0005221	-0.0003496
m7	0.02343	0.008249
m8 [K^{-1}]	0.00006741	0.0004796
m9	-1.208	0

In Tab. 2, materials properties used for the numerical simulation are reported.

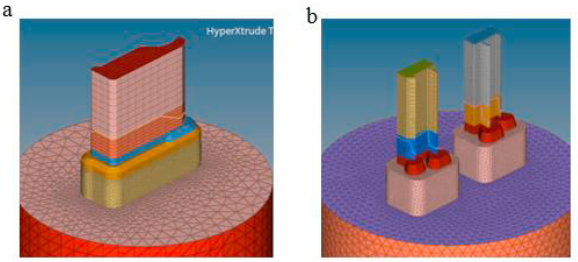

Fig. 13. Geometry meshed: (a) profile 1, (b) profile 2.

Table 2. Material properties.

Material Properties	Profile 1	Profile 2
Density [Kg/m^3]	2701	2690
Specific heat [J/kg K]	900	900
Thermal conductivity [W/m K]	180	200
Thermal expansivity [m/K]	2.34*10^{-5}	2.34*10^{-5}
Young's modulus [GPa]	68.9	68.9
Poisson's ratio	0.33	0.33

All the simulations were made by transient analyses with moving boundaries. In this kind of simulation, the mesh of profile, bearing, portholes and welding chamber remain fixed while, for the billet component, the elements are compressed and distorted according to the ram extrusion direction at each time step. A variable number of time steps were set in order to increase the accuracy of the analyses.

3.2. Analytical prediction and numerical results compared to the experimental data

In Tab. 4, results of experiments, numerical simulation and the other discussed methods are reported. Concerning the charge weld evolution, the defect is considered ended when, on the section of the extruded profile, the percentage of new billet is over 99.5%.

Table 4. Results analysis.

	Extents (distance from stop mark)	Profile 1	Profile 2
Experimental	Skin contamination onset [mm]	-3700	missing
	Charge welds end [mm]	+500	+900
Numerical	Skin contamination onset [mm]	-4538	-3750
	Charge welds end [mm]	+530	+950
Industrial Experience	Skin contamination onset [mm]	-4500	-2114
	Charge welds end [mm]	+1500	+1500
Theoretical (1)	Charge welds end [mm]	+133	+240
Theoretical (2)	Charge welds end [mm]	+199	+361
Empirical (3)	Skin contamination onset [mm]	-2155	-3320

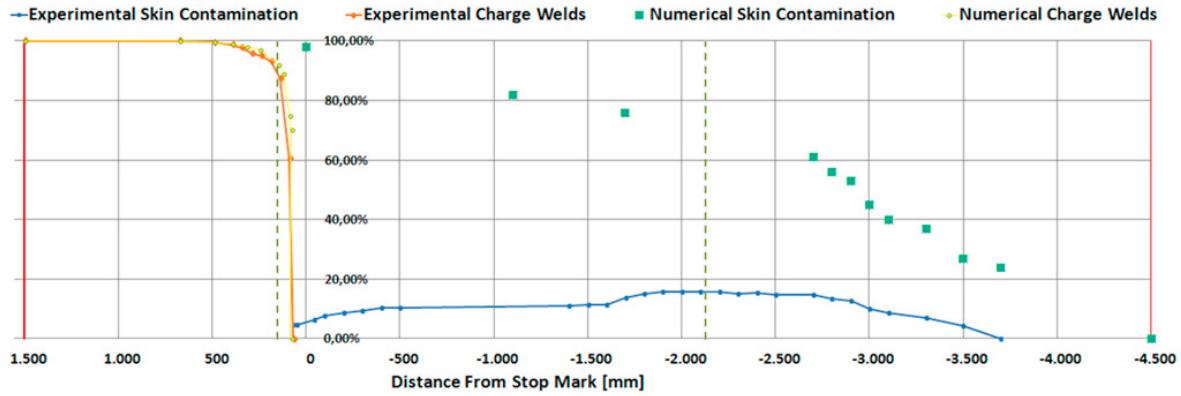

Fig. 14. Profile 1: charge welds and skin contamination evolutions from experimental and numerical analysis. Vertical red lines represent the scrap removed by the extrusion company, green dashed lines the scrap calculated by formula (2) and (3).

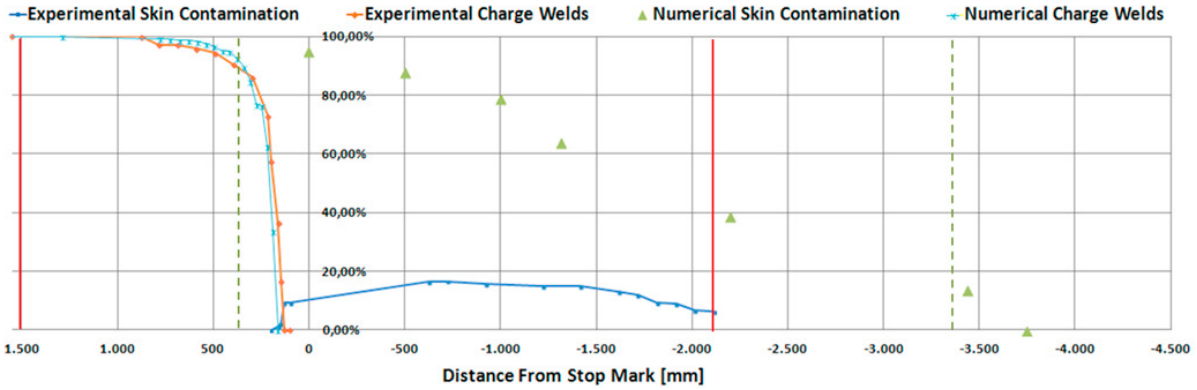

Fig. 15. Profile 2: charge welds and skin contamination evolutions from experimental and numerical analysis. Vertical red lines represent the scrap removed by the extrusion company, green dashed lines the scrap calculated by formula (2) and (3).

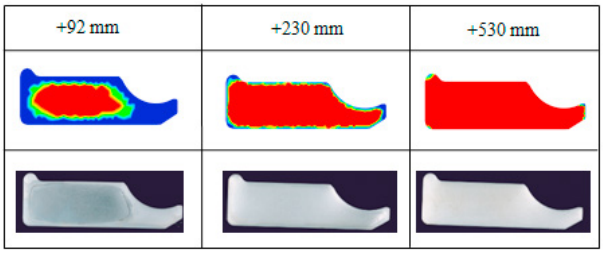

Fig. 16. Profile 1: comparison between charge welds experimental and numerical data at three different distances from the stop mark.

In Fig. 14 and Fig. 15 numerical and experimental charge welds and skin contamination evolutions [%] are shown and compared to the industrial scrap and to formulae (2) and (3) predictions.

Numerical simulations provided a very good prediction of charge welds evolution for both profile 1 (6 % error) and profile 2 (5,6% error) thus further confirming the achievements reported in literature. Theoretical formula (2) provided a deep underestimation of the extent (-60%) for both profiles, while the scrap based on industrial experience showed a relevant overestimation (+200% for profile 1 and +67% for profile 2).

The comparison shows the accuracy and flexibility of the simulation code on charge welds extent analysis. A further confirmation of the accuracy of the simulation prediction is evidenced by the good correlation between experimental and numerical data on billet replacement within the profile cross section. An example is reported in Fig.16: the Figure shows the numerical/experimental comparison of the material replacement on profile 1: charge welds defect starts from the center of the profile at 70 mm from stop mark then enlarging up to filling all the profile section at 500 mm.

Concerning the skin contamination prediction, the considerations are quite different. It has to be reminded that skin contamination onset was experimentally determined for profile 1 only (-3700 mm), since the company scrapped the profile 2 at -2114 mm from the stop mark where the defect was already present. Anyhow some important considerations can be drawn anyway:

- for profile 1, the numerical simulation predicted the onset of the skin contamination at -4538 mm from the stop mark, while experimentally onset was found at -3750 mm (overestimation of 16%);

- the simulation always shows higher values of percentage of skin contamination evolution on the section of the profile in relation to experimental ones (both profile 1 and 2). As discussed before, this behavior is probably programmed in the FEM code in relation to the general knowledge that billet skin contamination has to evolve to a 100 % replacement independently from charge welds;
- for profile 2, although the starting point of the billet skin contamination is not known, the simulations outputs are not in contrast with experimental data;
- empirical relation (3) provided an underestimated value of defect onset on profile 1 (-42%) while for profile 2 the predicted value is not too far from the numerical one.

4. Conclusions

In the present work, experimental and numerical campaigns were carried out for evaluating the accuracy of Altair HyperXtrude FEM code and other methods available in literature in the prediction of charge welds and skin contamination evolution. The studies were performed on two solid profiles made by AA6063 and AA6082 aluminum alloy.

The main outcomes of this work can be summarized as followed:

- a good correlation between experimental and numerical data on charge welds prediction, both in terms of extent and of percentage evolution, was confirmed also in this study in the two investigated profiles;
- concerning the skin contamination onset, the numerical result shows the beginning at -4538 mm from the stop mark instead of the experimental value of -3750 mm (16 % error);
- concerning skin contamination evolution (percentage over stroke), in the numerical simulation values up to 100% were reached while experimental evidence shows maximum values of 15-20%;
- theoretical and empirical formulae deeply underestimate the evolution of both front and back-end defects (-60% and -42% respectively);
- some more effort for an improvement of the accuracy of billet skin contamination prediction is required including some studies on simulation parameters (mesh dimensions, friction coefficients, etc) but probably also in term of code development;
- anyhow, from an industrial point of view, it has be noted that the overestimation of percentage of skin contamination is not a concern since the profile has to be scrapped anyway whilst the overestimation of the onset point of the contamination is ‘precautionary’ from a production point of view; in other words, although not fully accurate, the FEM simulations can already provide an indication on billet skin evolution for a selected die design.

References

[1] Sheppard T. Extrusion of Aluminum Alloy. Springer; 1999.
[2] Kim YT, Ikeda K. Flow behavior of billet surface layer in porthole die extrusion of aluminum. Metall Mater Trans A 2000; 31(6):1635-1643.
[3] Reggiani B, Donati L. Experimental, numerical and analytical investigations on the charge weld evolution in extruded profiles. Int J of Advanced Manufacturing Technology 2018; 99(5-8):1379–1387.
[4] Saha P. Quality issues of hollow extrusions for aerospace applications. Proc. of the 9th Extrusion Technology Seminar 2008; Florida, US.
[5] Kathirgamanathan P, Neitzert T. Optimization of pocket design to produce a thin shape complex profile. Prod. Eng. Res. Devel 2009; 3:231–241.
[6] Reggiani B, Donati L, Tomesani L. ICEB - International conference on extrusion and benchmark. Light Metal Age 2017; 75(5):52-60.
[7] Li L, Zhang H, Zhou J, Duszczyk J, Li G, Zhong ZH. Numerical and experimental study on the extrusion through a porthole die to produce a hollow magnesium profile with longitudinal weld seams Mater Des 2008; 29:1190-1198.
[8] Reggiani B, Donati L, Tomesani L. Multi-goal optimization of industrial extrusion dies by means of meta-models. Int. J. Adv. Man. Tech. 2017; 88(9-12):3281-3293.
[9] Finkelnburg WD, Scharf G. Some investigation on the metal flow during extrusion of Al alloys. In the proc. of the 5th Extrusion Technology Seminar, 1992; Chicago, USA.
[10] Kim YT, Ikeda K. Flow Behavior of the Billet Surface Layer in Porthole Die Extrusion of Aluminum. Met. Mater. Trans. A 2000; 31A:1635-1643.
[11] Jowett C, Adams J, Daughetee C, Lea G, Huff OA, Fossl N. Scrap allocation. In the Proc. of the 9th Extrusion Technology Seminar 2008; Florida, USA.
[12] Ishikawa T, Sano H, Yoshida Y, Yukawa N, Sakamoto J, Torzawa Y. Effect of Extrusion Conditions on Metal Flow and Microstructures of Aluminum Alloys, CIRP Annals 2006; 55 (1):275-278.
[13] Hatzenbichler T., Buchmayr B. Finite element method simulation of internal defects in billet-to-billet extrusion, Proc. of the Institution of Mechanical Engineers, Part B: Journal of Engineering Manufacture 2010; 224:1029-1042.
[14] Jowett C, Parson N, Fraser W, Hankin J, Hicklin K. Simulation of Flow of the Billet Surface into the Extruded Product. In the Proc. of the 7th Extrusion Technology Seminar I 2000; 27–42.
[15] Lou S, Wang Y, Liu C, Lu S, Lu S, Su C. Analysis and Prediction of the Billet Butt and Transverse Weld in the Continuous Extrusion Process of a Hollow Aluminum Profile J. of Materi Eng and Perform 2017;26:4121-4130.
[16] Hensel A, Spittel T. Kraft und Arbeitsbedarf bildsamer Formgeburgsverfahren, 1. Auflage, VEB DeutscherVerlag fur Grundstoffindustrie 1978; Leipzig.
[17] El Mehtedi M, Spigarelli S, Gabrielli F, Donati L. Comparison study of constitutive models in predicting the hot deformation behavior of AA6060 and AA6063 Aluinum alloys. Materials Today: Proceedings 2015; 2(10):4732–4739.
[18] Selvaggio A, Kloppenborg T, Schwane M, Hölker R, Jäger A, Donati L, Tomesani L, Tekkaya AE. Extrusion benchmark 2013 - Experimental analysis of mandrel deflection, local temperature and pressure in extrusion dies, Key Engineering Materials 2014; 585:13-22